

Supporting Information for Manuscript Entitled with
**Facile preparation of bio-based polyesters from
furandicarboxylic acid and long chain diols *via* asymmetric
monomer strategy**

Yong Shen^a, Binbin Yao^b, Guang Yu^b, Yao Fu^c, Fusheng Liu^{a,*} and Zhibo Li^{b,*}

^a College of Chemical Engineering, Qingdao University of Science and Technology, Qingdao 266042, P.R. China.

^b Key Laboratory of Biobased Polymer Materials, Shandong Provincial Education Department; School of Polymer Science and Engineering, Qingdao University of Science and Technology, Qingdao 266042, P.R. China.

^c Anhui Province Key laboratory of Biomass Clean Energy, Department of Chemistry, University of Science and Technology of China, Hefei 230026, P.R. China.

Corresponding authors: E-mail: liufusheng63@sina.com;

E-mail: zbli@qust.edu.cn

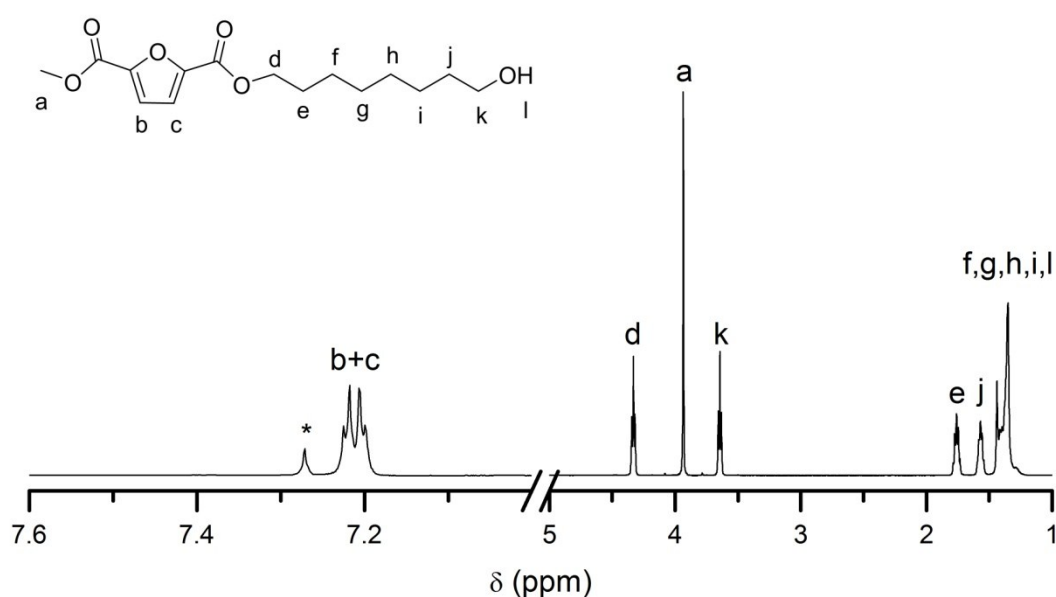


Figure S1. ¹H NMR spectrum of mmFDCA-oct-ol (* represents the residual deuterated solvent peak).

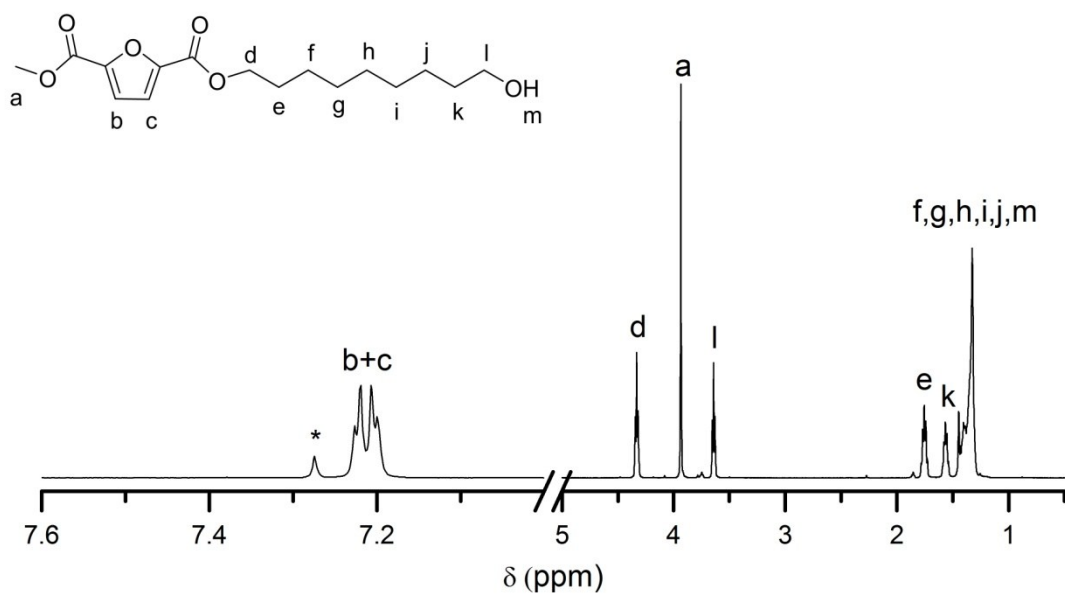


Figure S2. ^1H NMR spectrum of mmFDCA-non-ol (* represents the residual deuterated solvent peak).

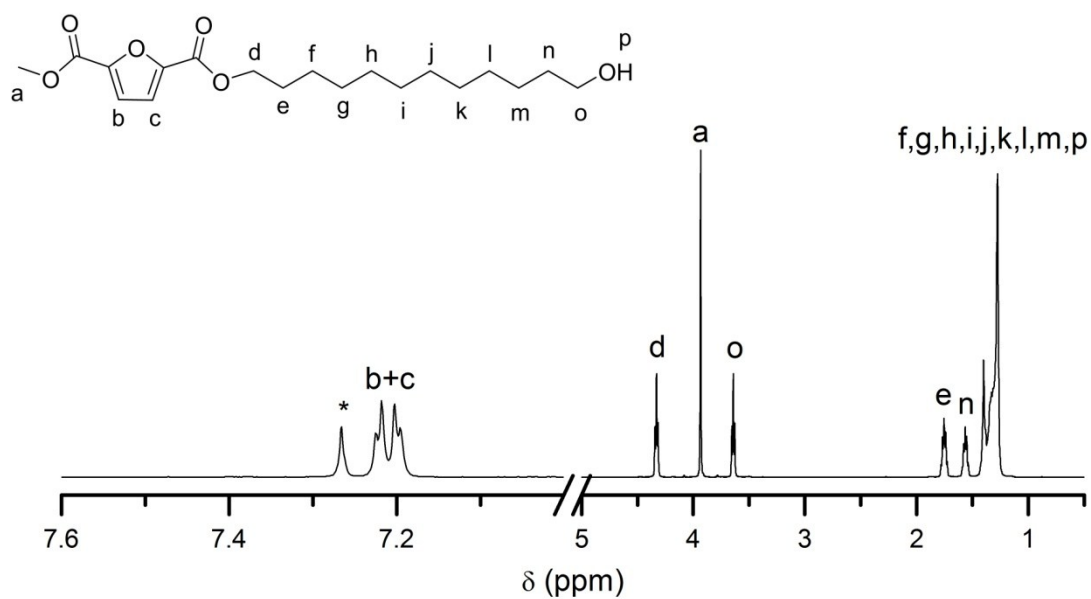


Figure S3. ^1H NMR spectrum of mmFDCA-dod-ol (* represents the residual deuterated solvent peak).

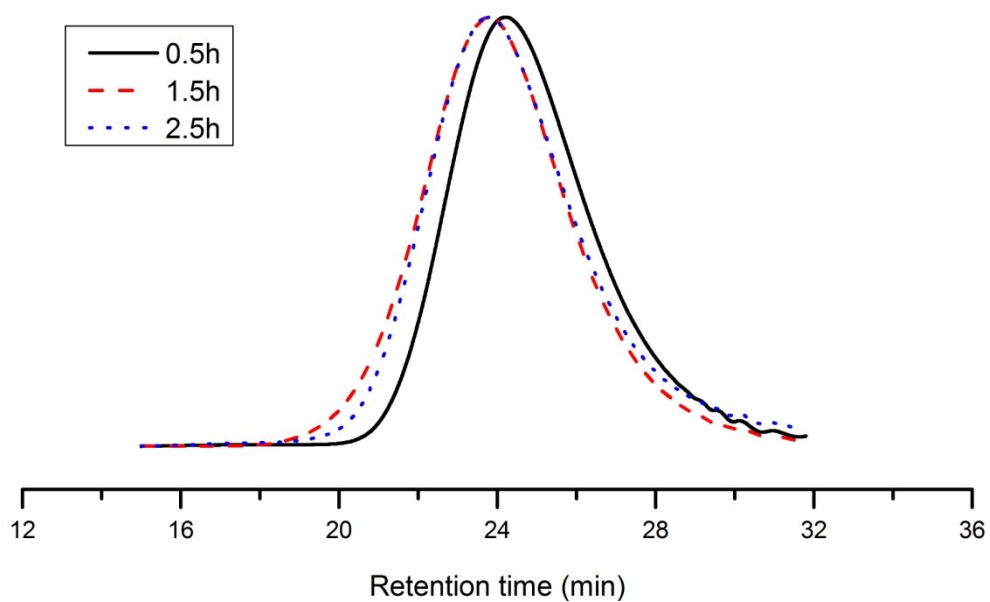


Figure S4. SEC traces of PdecF samples prepared at different time.

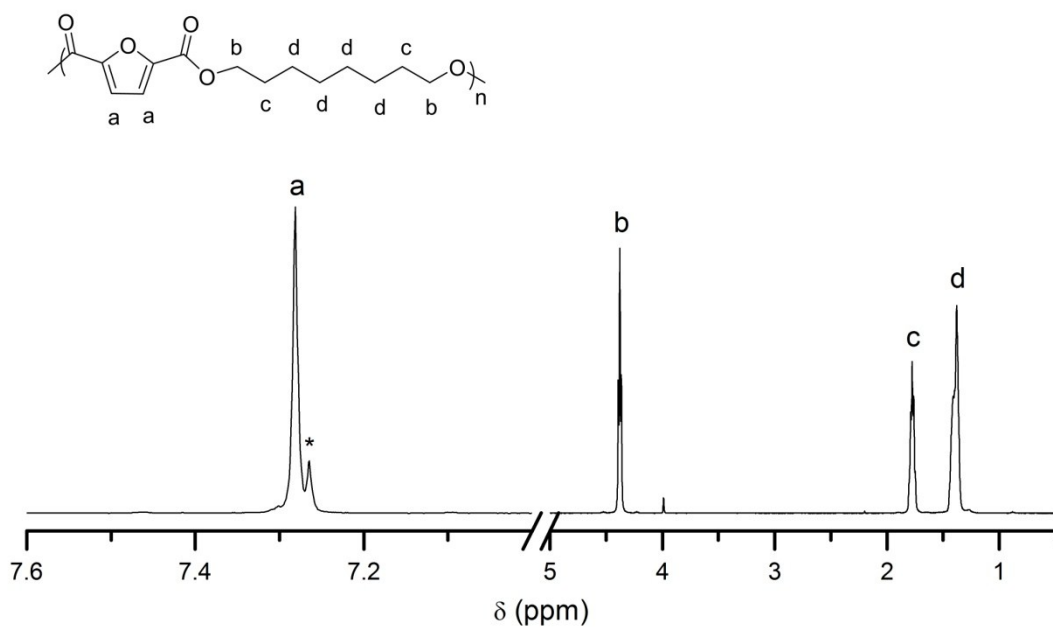


Figure S5. ^1H NMR spectrum of POF (* represents the residual deuterated solvent peak).

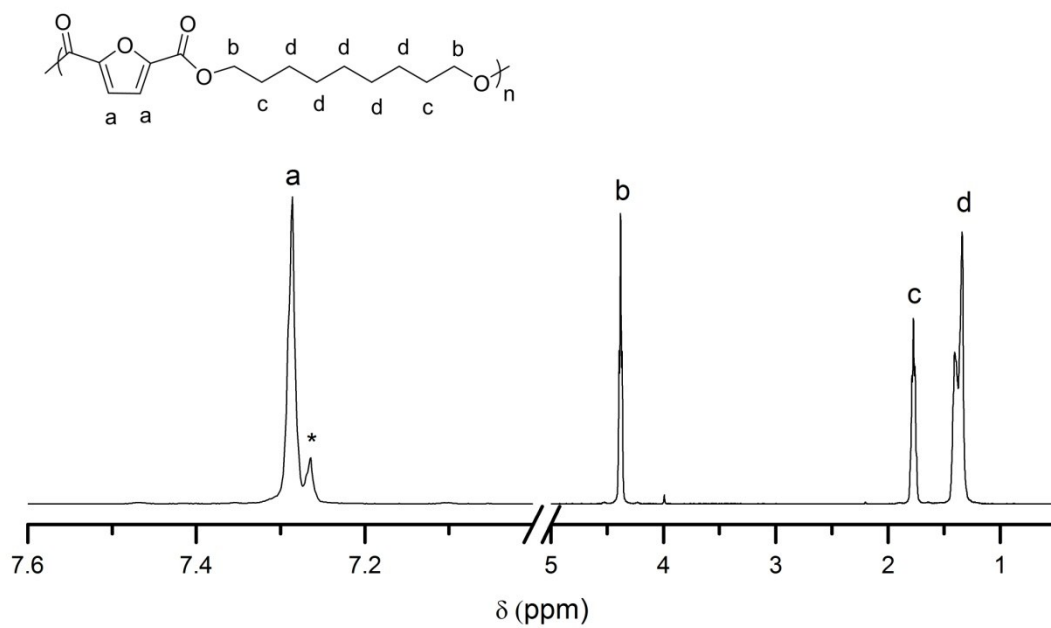


Figure S6. ^1H NMR spectrum of PNF (* represents the residual deuterated solvent peak).

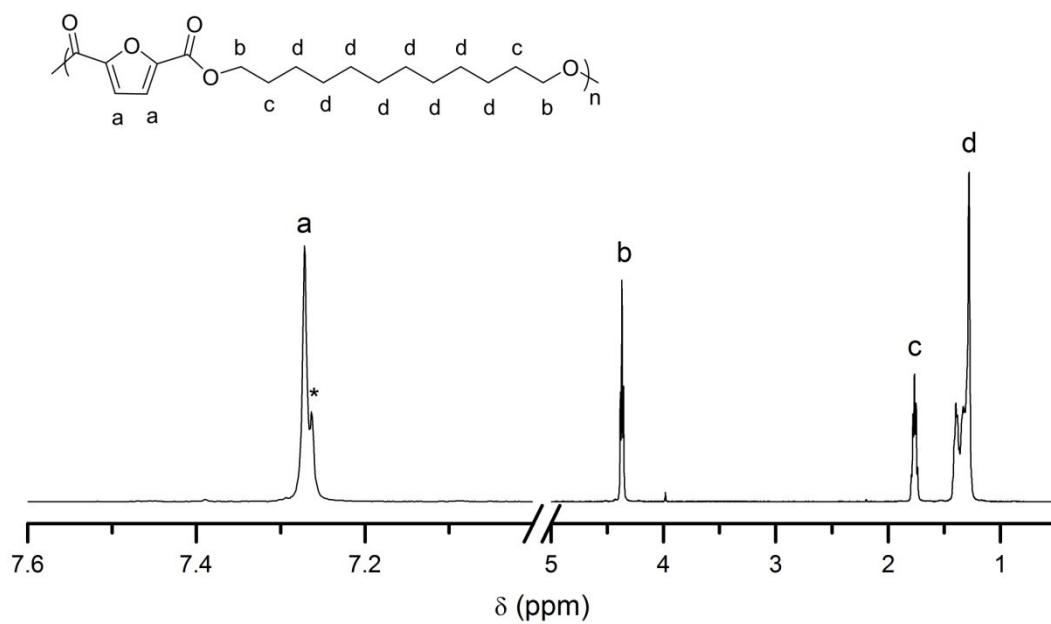


Figure S7. ^1H NMR spectrum of PdodF (* represents the residual deuterated solvent peak).

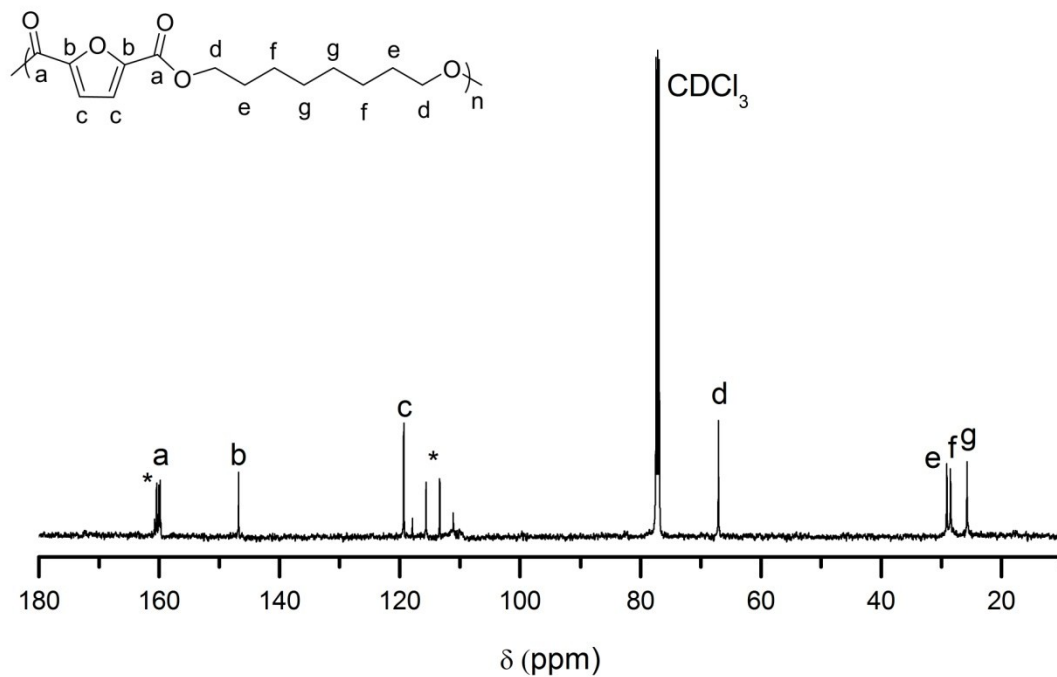


Figure S8. ¹³C NMR spectrum of POF (* represents the residual CF₃COOD peak).

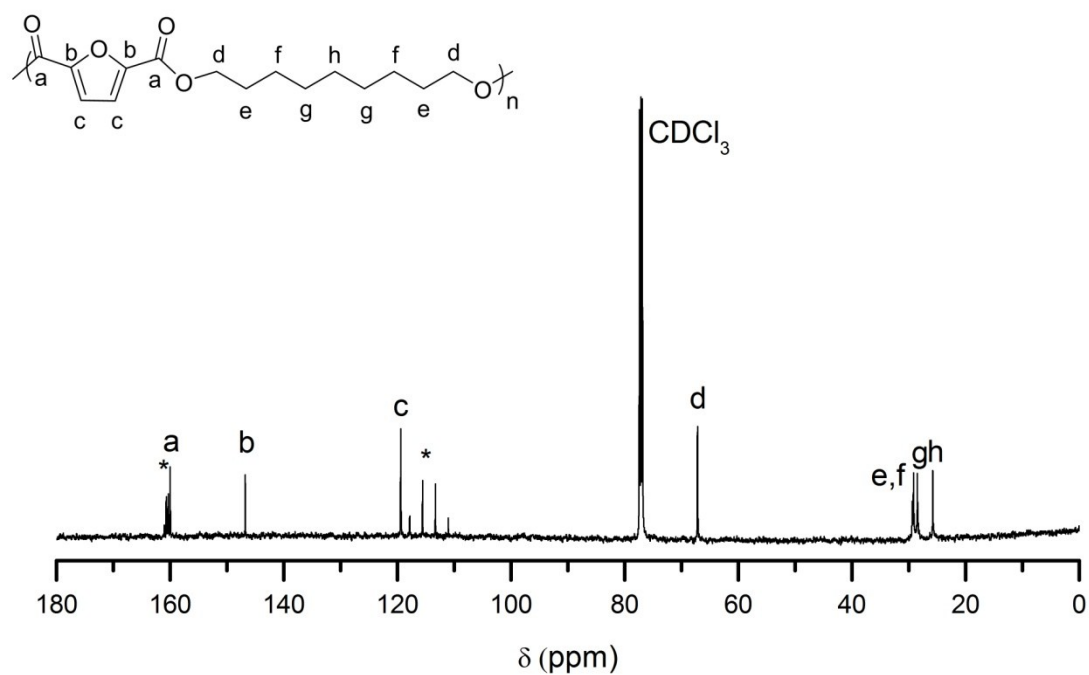


Figure S9. ¹³C NMR spectrum of PNF (* represents the residual CF₃COOD peak).

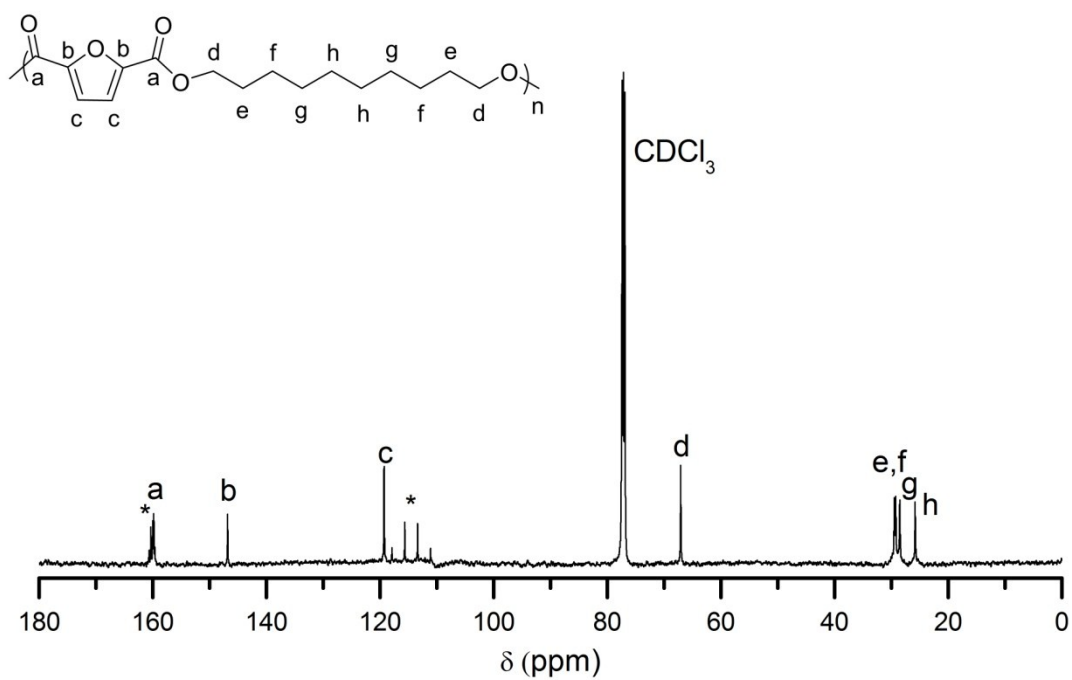


Figure S10. ¹³C NMR spectrum of PdecF (* represents the residual CF₃COOD peak).

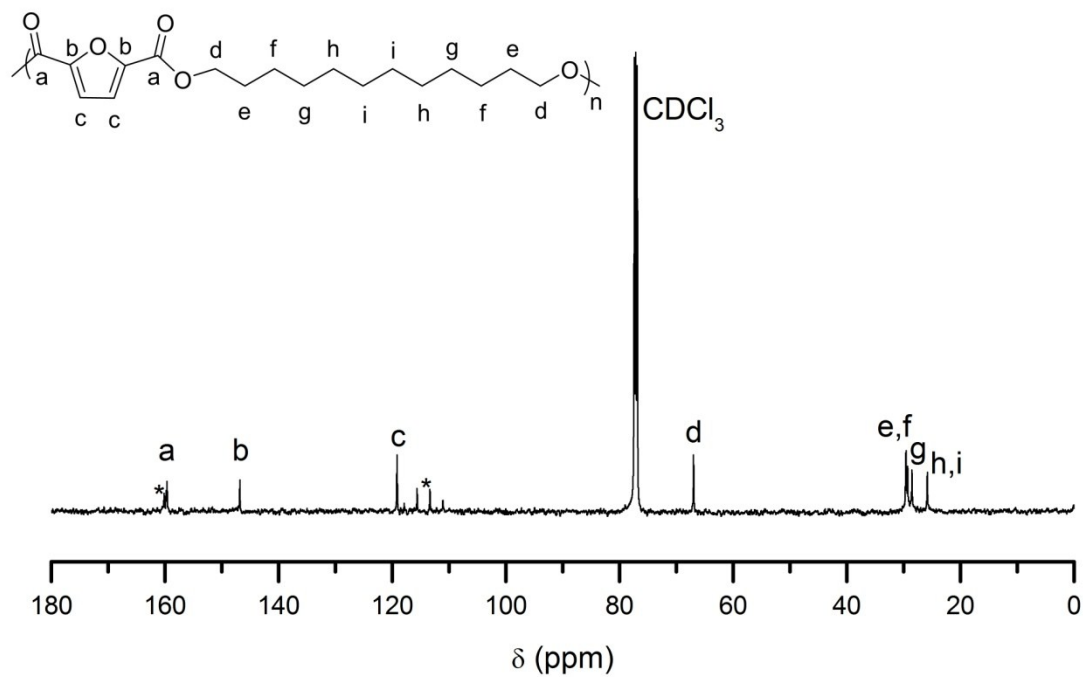


Figure S11. ¹³C NMR spectrum of PdodF (* represents the residual CF₃COOD peak).

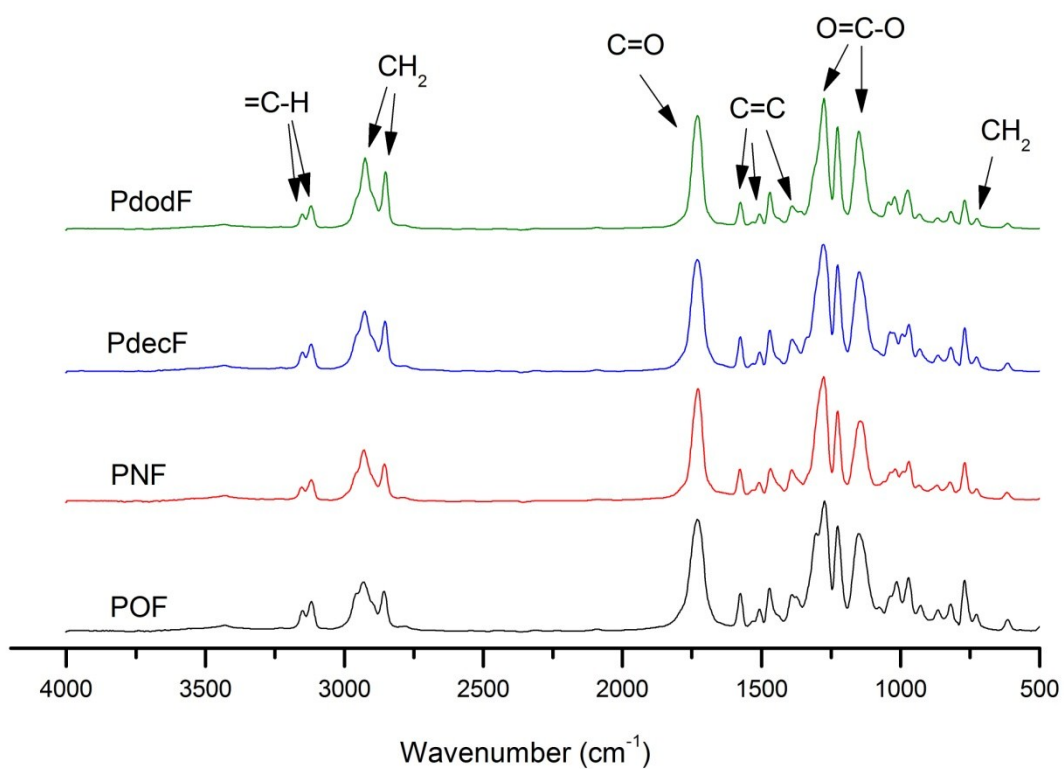


Figure S12. FTIR spectra of POF, PNF, PdecF and PdodF.

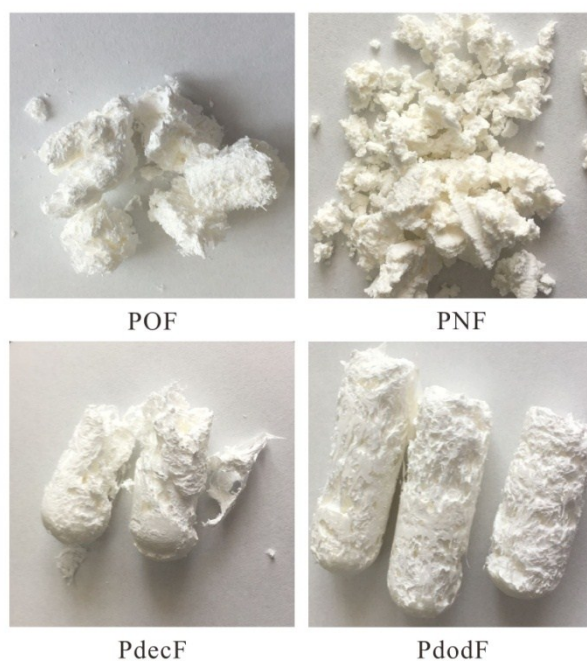


Figure S13. Photos of the obtained polyesters.

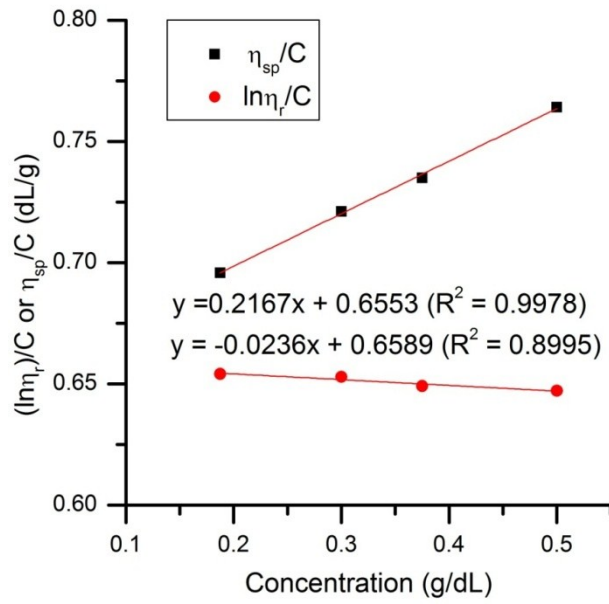


Figure S14. Determination of intrinsic viscosity of POF.

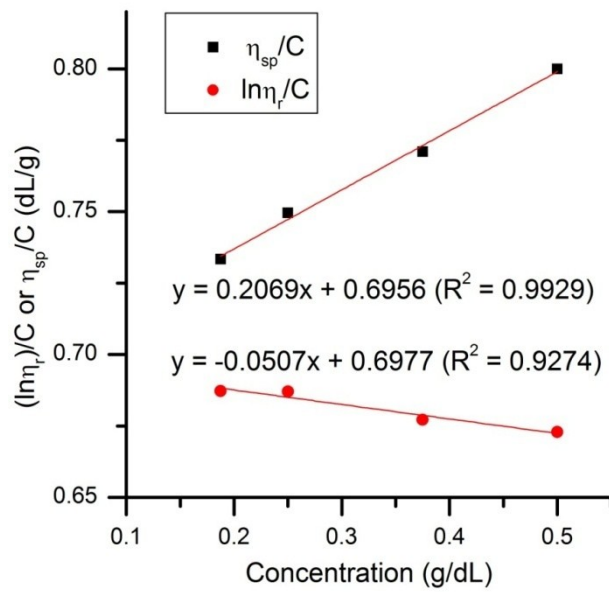


Figure S15. Determination of intrinsic viscosity of PNF.

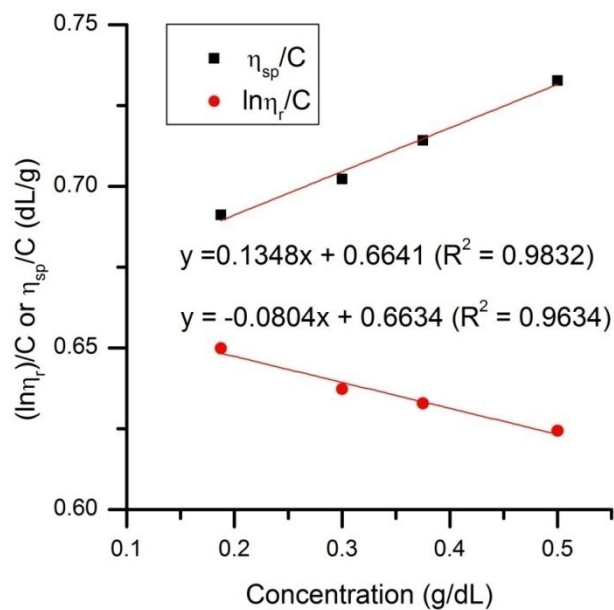


Figure S16. Determination of intrinsic viscosity of PdecF.

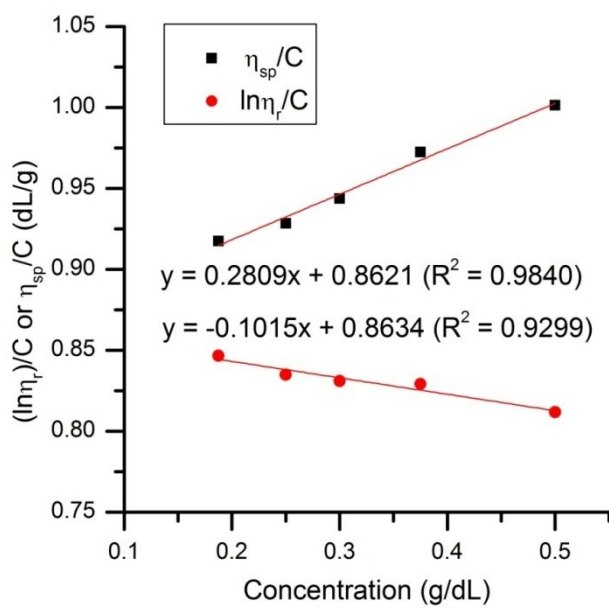


Figure S17. Determination of intrinsic viscosity of PdodF.

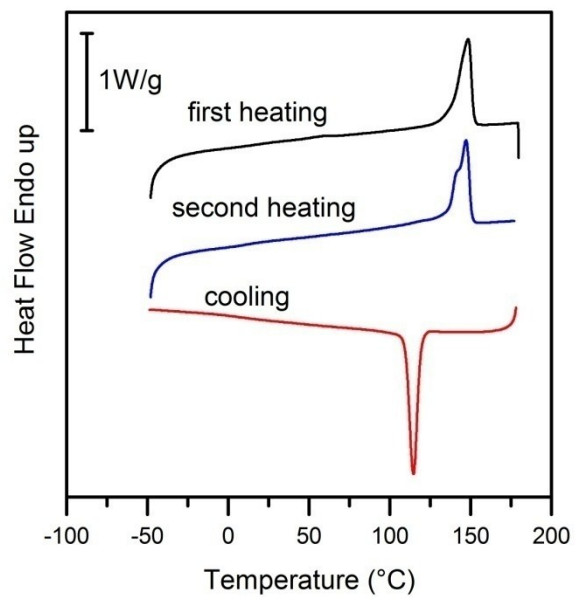


Figure S18. DSC scans of POF.

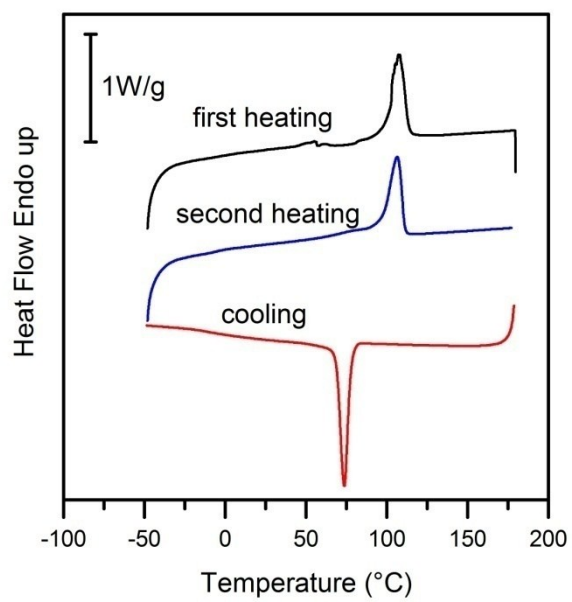


Figure S19. DSC scans of PdodF.

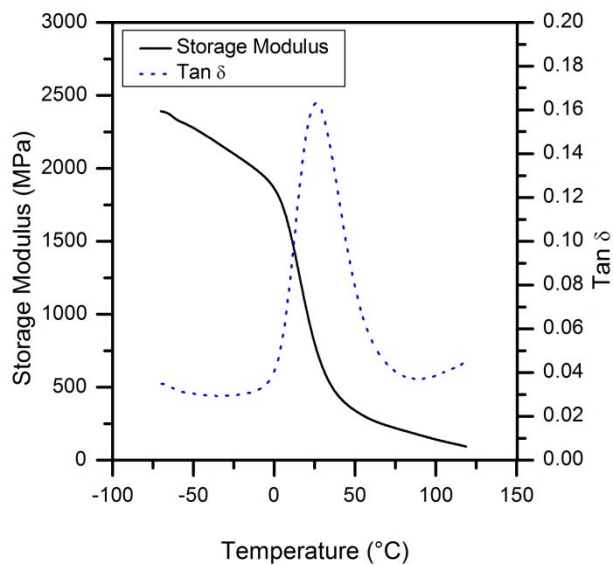


Figure S20. Storage modulus and $\tan\delta$ of POF as a function of temperature obtained with DMA.

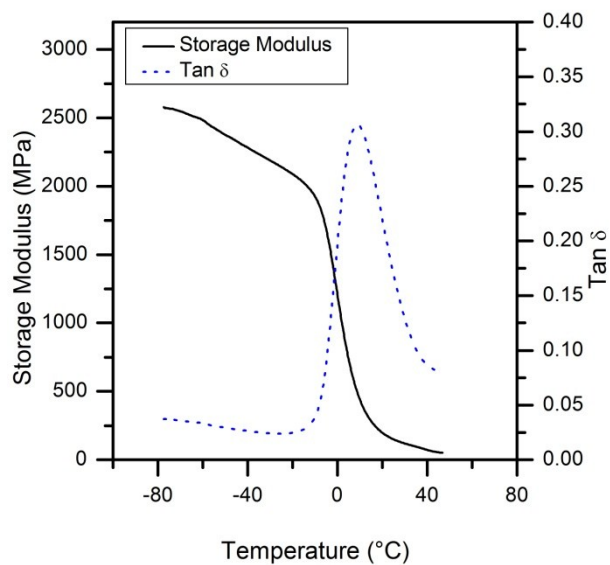


Figure S21. Storage modulus and $\tan\delta$ of PNF as a function of temperature obtained with DMA.

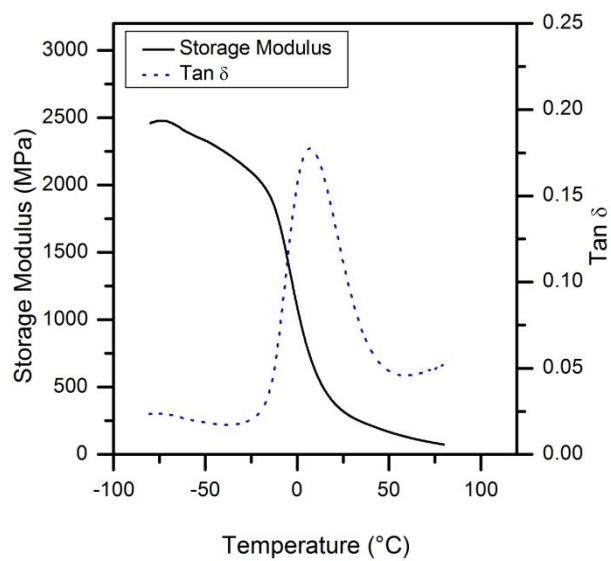


Figure S22. Storage modulus and $\tan\delta$ of PdodF as a function of temperature obtained with DMA.

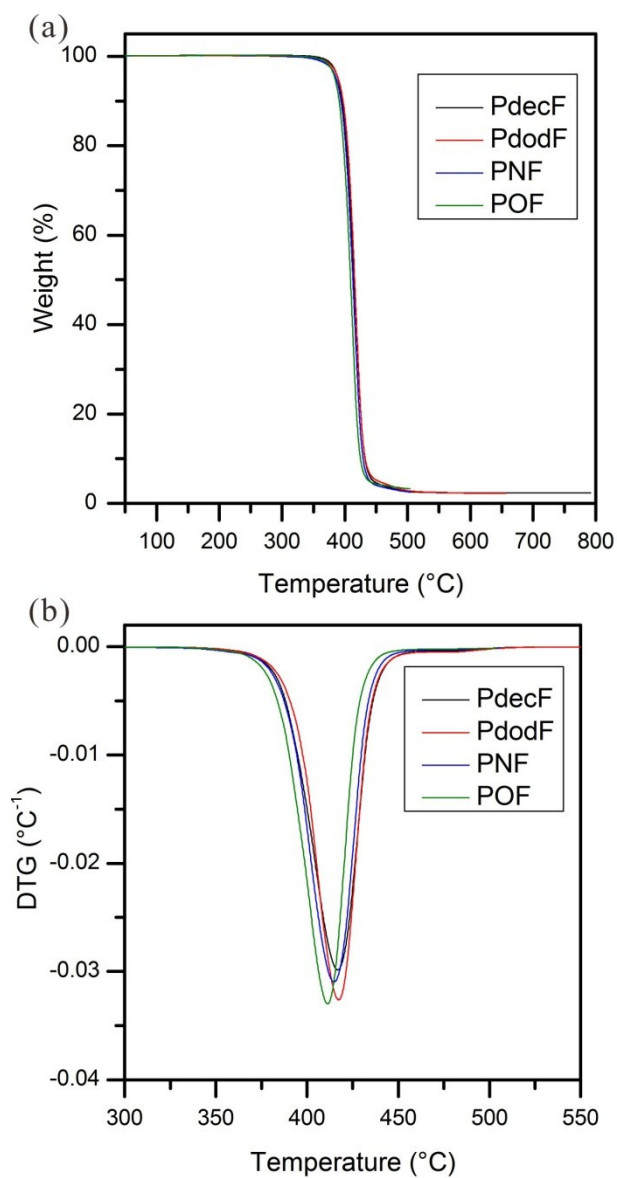


Figure S23. (a) Weight loss and (b) differential thermal gravity (DTG) curves obtained with TGA.

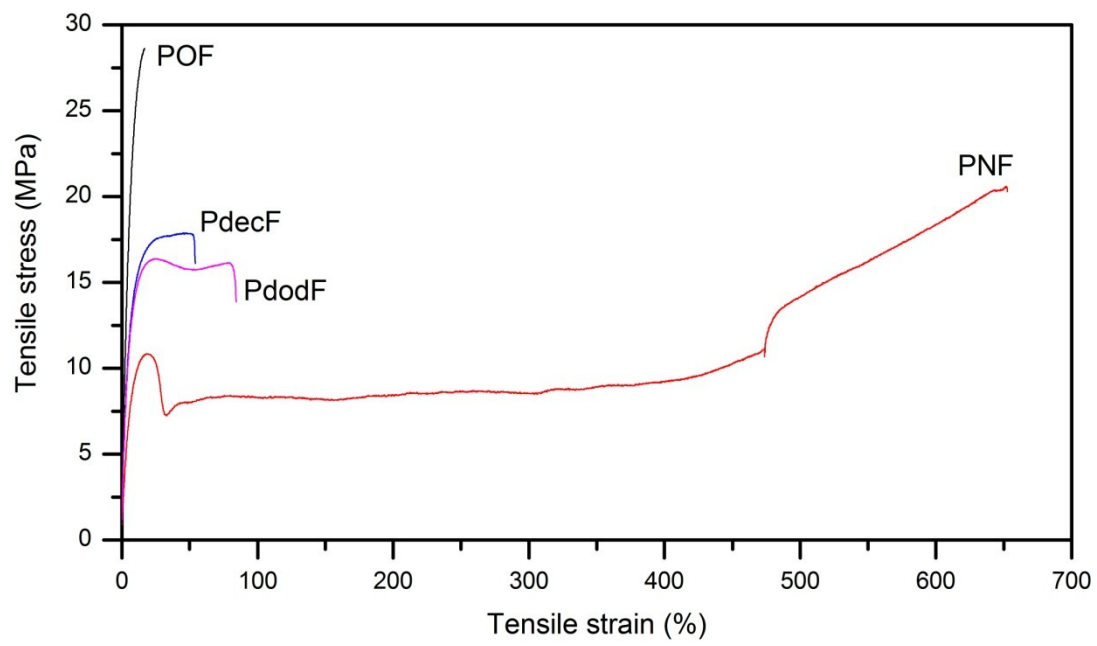


Figure S24. Stress-strain curves of POF, PNF, PdecF and PdodF.